Cell Reports Physical Science, Volume *1*

Supplemental Information

Domain Wall Conduction in Calcium-Modified Lead Titanate for Polarization Tunable Photovoltaic Devices

Chong-Xin Qian, Hong-Jian Feng, Qiang Zhang, Jiawei He, Zi-Xuan Chen, Ming-Zi Wang, and Xiao Cheng Zeng

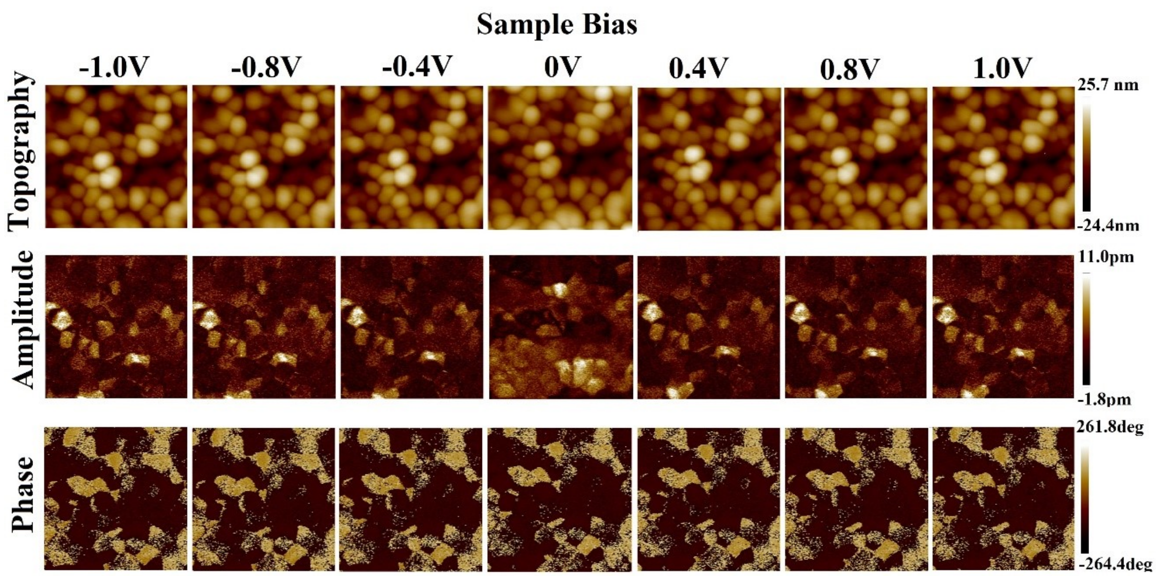

Figure S1. The PCT film surface topography, amplitude and the phase images under the bias voltage arrange from 0 to ± 1V, respectively.

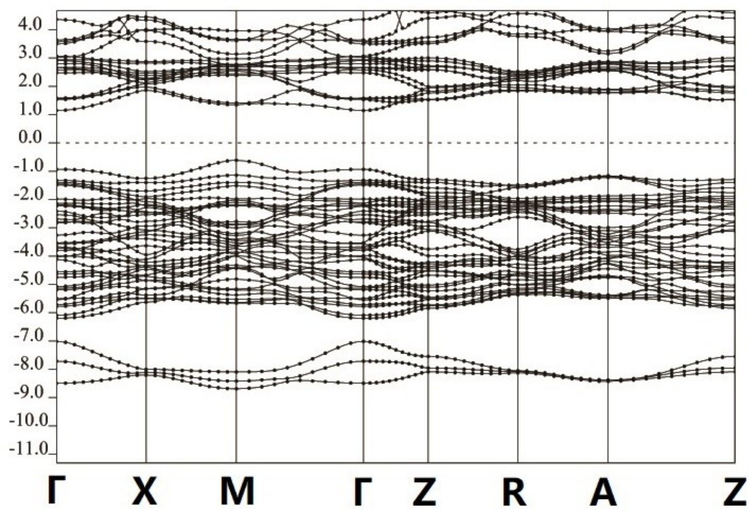

Figure S2. Computed electronic band structure calculated by PBE/GGA.

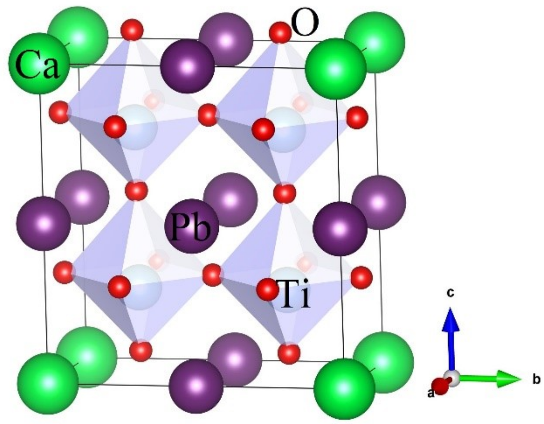

Figure S3. The $Pb_{0.8}Ca_{0.2}TiO_3$ cell structure.

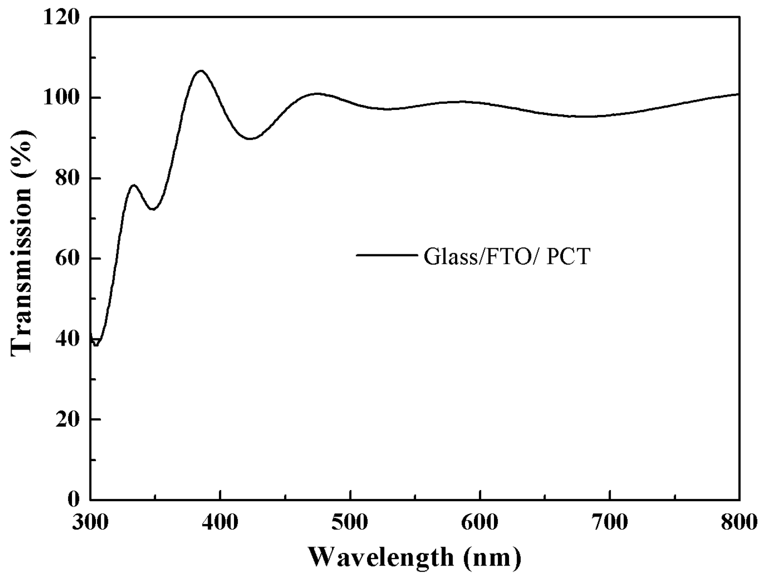

Figure S4. Optical transmission spectra of PCT film.

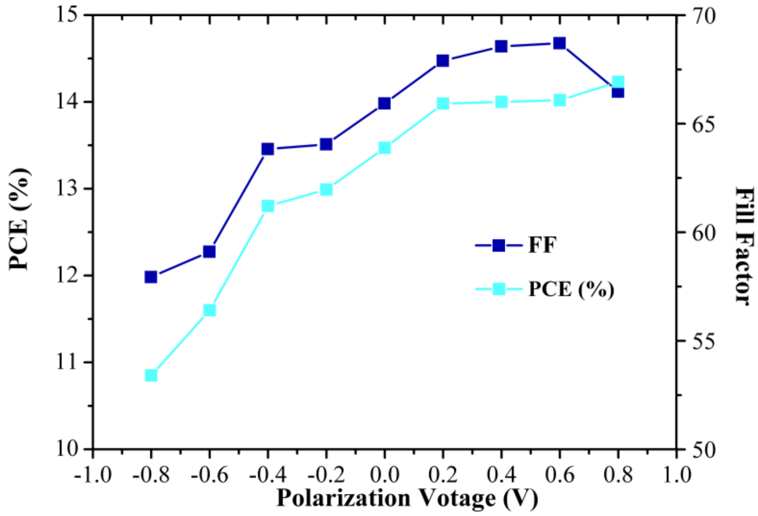

Figure S5. The PCE and the Fill Factors measured after poling with different polarization bias.

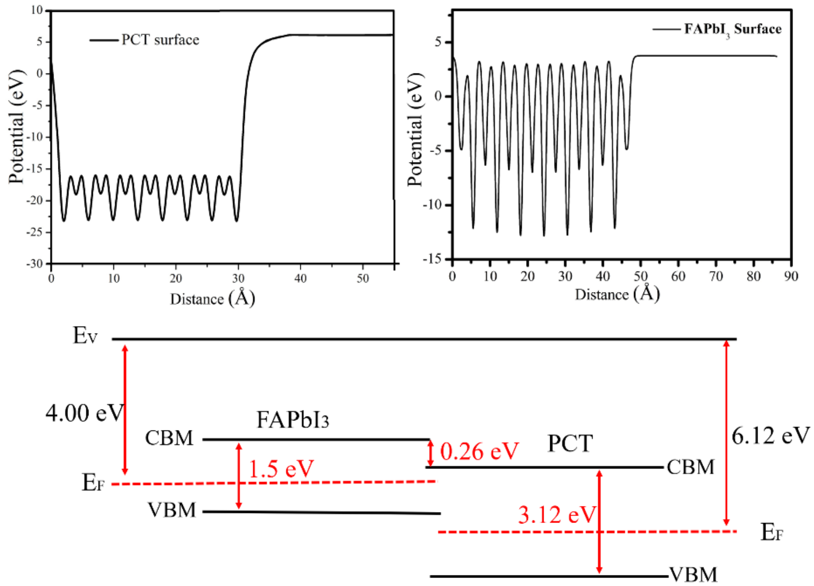

Figure S6. Conduction band offset schematic of $FAPbI_3$/PCT heterostructure based on work functions computed based on HSE06 functional with respect to the vacuum level.

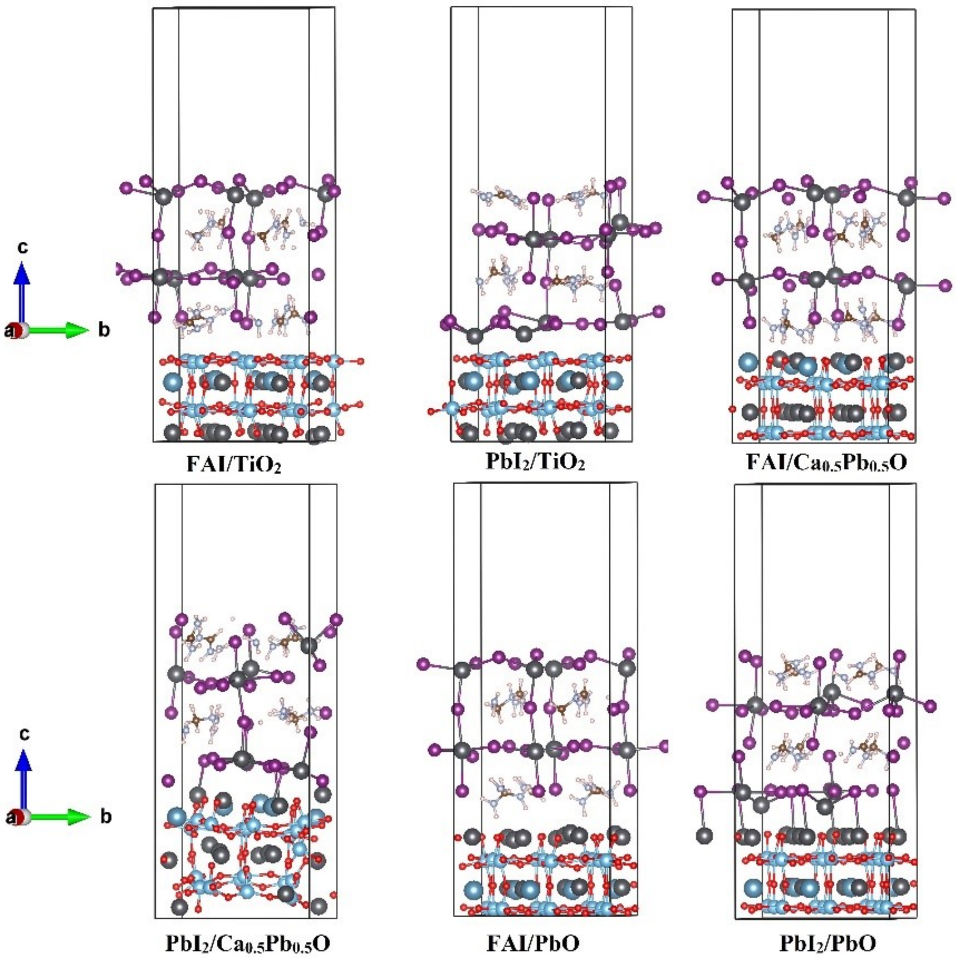

Figure S7. Six different relaxed interfaces for PCT/perovskite heterojunction.

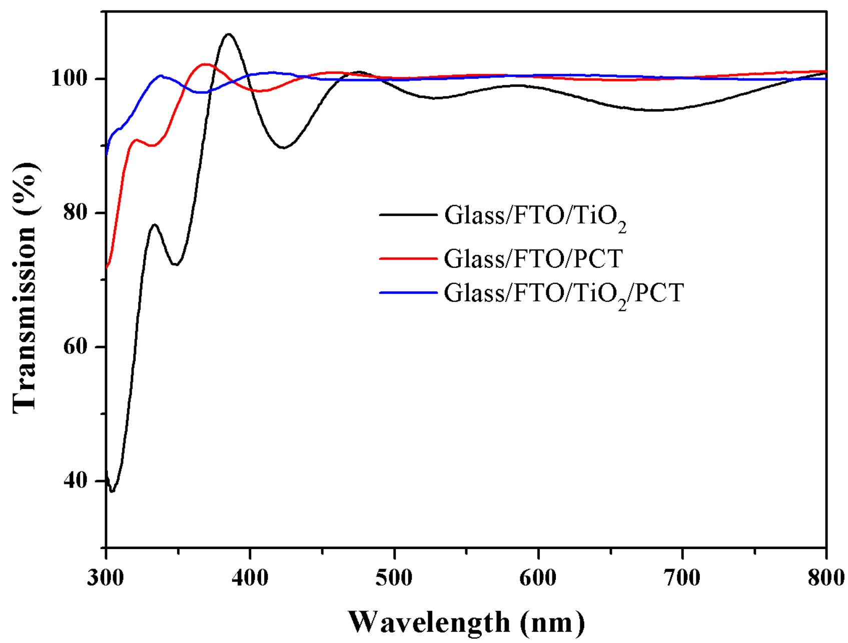

Figure S8. Measured transmission of different ETLs deposited on Glass/FTO substrate.

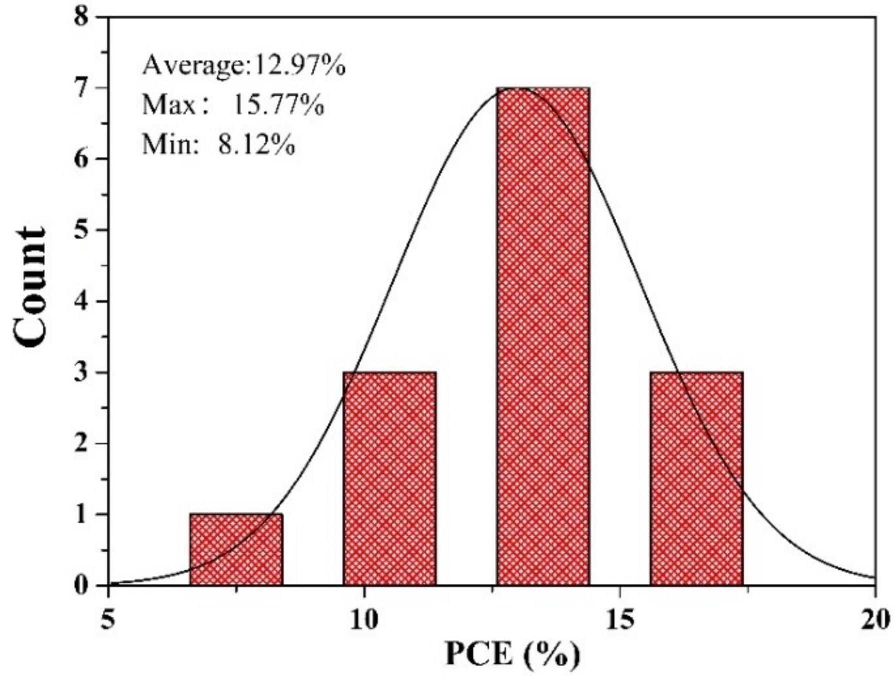

Figure S9. The histogram of the PCE of the passivated PCT-based devices.

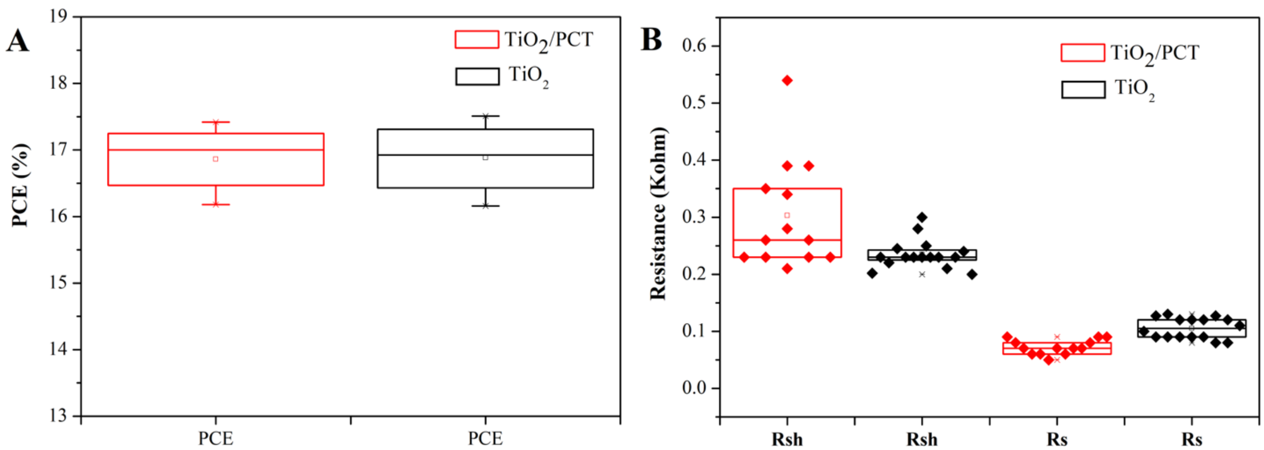

Figure S10. Statistics of the device performance PCE (A) and (B) the series resistance (R_s) and shunt resistance (R_{sh}) of PSCs with TiO_2 and TiO_2/PCT as ETLs, respectively. The median and mean are represented by the line dividing the boxes and the open square symbols, respectively. The cross symbols represent the maximum and minimum values.

Table S1. Upon the different poling bias, the parameters measured from reverse direction of PCT based device.

Poling bias	**V_{oc}(V)**	**J_{sc}(mA/cm^2)**	**FF(%)**	**PCE(%)**
Poling +0.8V	1.08	23.16	63.91	15.98
Poling +0.6V	0.98	21.80	66.48	14.08
Poling +0.4V	1.04	19.59	66.42	13.53
Poling +0.2V	0.98	20.85	65.93	13.47
No Poling	0.98	20.70	64.05	12.99
Poling -0.2V	0.98	20.56	63.83	12.85
Poling -0.4V	0.96	20.45	59.11	11.60
Poling -0.6V	0.94	19.92	57.94	10.85
Poling -0.8V	0.96	17.01	51.61	8.43

Table S2. The key parameters of different ETL devices.

ETL		V_{oc}(V)	J_{sc} (mA/cm^2)	FF (%)	PCE (%)
TiO_2	Reverse	1.1	20.74	76.74	17.51
	Forward	1.04	20.78	69.96	15.12
PCT	Reverse	1.08	23.16	63.91	15.99
	Forward	0.98	23.05	66.39	14.99
TiO_2/ PCT	Reverse	1.05	23.11	75.29	18.28
	Forward	1.04	22.81	68.73	16.34

Supplemental Experimental Procedures

Materials

Lead acetate trihydrate, calcium acetate, tetrabutyl titanate, ethylene glycol monomethyl ether, diacetone, formamide, acetic acid and titanium tetrachloride were purchased from Sinopharm Chemical Reagent Co. Ltd. MAI (99.99%), FAI (99.99%), PbI_2 (99.9985%), 2,2,7,7-Tetrakis (N,N-di-p-methoxyphenylamine)-9,9-spirobif-luorene (Spiro-OMeTAD), Lithium bis (trifluoro-methanesulfonyl) imideanhydrous (Li-TFSI) and 4-tertbuthylpyridine (tBP) were purchased from Xi'an Poled Electronic Technology Co. Ltd. CsI, $PbBr_2$, acetonitrile and chlorobenzene were purchased from Aladdin. All precursor materials and solvents were used as received without further purification.

The charge displacement curve between the lowest triplet states and the ground states

The charge displacement curve (CDC)

The plane-averaged charge difference Δq can be defined by

$$\Delta q = \int_{-\infty}^{+\infty}\int_{-\infty}^{+\infty}(\rho_{FA/BTO} - \rho_{FA} - \rho_{BTO})dxdy \tag{1}$$

Where $\rho_{FA/BTO}$, ρ_{FA} and ρ_{BTO} are charge density of $FAPbI_3$/BTO heterostructure, $FAPbI_3$ slab and BTO slab, respectively. The CDC curve can be calculated by integrating Δq along z axis

$$\Delta Q = \int_{-\infty}^{z}\Delta q dz \tag{2}$$

The CDC curve between the lowest triplet states and the ground states.

The CDC curve ΔQ between the lowest triplet states and the ground states can be calculated by

$$\Delta Q = \int_{-\infty}^{\infty}dx\int_{-\infty}^{\infty}dy\int_{-\infty}^{z}(\rho_L - \rho_G)dz \tag{3}$$

Where ρ_L and ρ_G denote the electron density of lowest triplet states and ground states in the real space, respectively.